

Kinetics and modeling of liquid–liquid phase transfer catalysed synthesis of *p*-chlorophenyl acetonitrile: role of co-catalyst in intensification of rates and selectivity

Ganapati D. Yadav^{*}, Yogeeta B. Jadhav

Department of Chemical Engineering, University Institute of Chemical Technology,
University of Mumbai, Matunga, Mumbai 400019, India

Received 5 February 2002; accepted 9 July 2002

Abstract

The role of a co-catalyst in the intensification of rates of liquid–liquid (L–L) phase transfer catalysed reaction is studied in allusion to the synthesis of *p*-chlorophenyl acetonitrile by using tetrabutylammonium bromide (TBAB) as the phase transfer (PT) catalyst and potassium iodide as the co-catalyst. Due to the co-catalytic action of potassium iodide, there is an intensification of reaction rates by orders of magnitude resulting from the in situ formation of a more active *p*-chlorobenzyl iodide and the selectivity is 100%. The catalyst is predominantly distributed in two forms, Q^+I^- and Q^+CN^- . A mechanistic model consistent with the kinetics of the process is described. The study provides a deeper insight into the complexities of the co-catalysed phase transfer catalytic (PTC) processes.

© 2002 Elsevier Science B.V. All rights reserved.

Keywords: Liquid–liquid phase transfer catalysis; Co-catalyst; *p*-Chlorophenyl acetonitrile; Potassium iodide; Reaction kinetics; Modeling

1. Introduction

The reaction between benzyl halides and alkali metal cyanides in polar solvents constitutes the classical and generally acceptable method for the synthesis of phenylacetonitriles. The polarity and nucleophilicity of the solvent and the basic nature of the cyanide ion do, however, lead to a number of anomalous reactions which limit the utility of the method. Phase transfer catalysis (PTC) proves to be an excellent alternative to this conventional method. Various types of phase transfer (PT) catalysts have been employed

for cyanide displacement on alkyl halides to yield nitriles. The cyanide displacement on *p*-chlorobenzyl halide has reportedly been done under liquid–liquid (L–L) PTC conditions by using different PT catalysts, such as triethylamine (which forms a quaternary ammonium salt in situ) [1], aliquat 336 [2], tetrabutylammonium chloride [3], triethylbenzylammonium chloride [4] and polystyrene supported PTC under triphase catalysis [5]. However, the mechanistic aspects of the reaction have not been adequately addressed. Also, most of the information available is patented.

In certain PTC reactions, co-catalysts have reportedly been used to enhance either the transfer rate or the intrinsic organic reaction rate. Use of two PT catalysts or use of alcohols or related compounds, metal compounds and iodide as co-catalysts is known to

^{*} Corresponding author. Tel.: +91-22-410-2121;
fax: +91-22-414-5614.
E-mail addresses: gdy@udct.ernet.in, gdyadav@yahoo.com
(G.D. Yadav).

Nomenclature

$[A]_0$	initial concentration of <i>p</i> -CBC in the organic phase (mol/cm ³)
k_{aq-1}	second order rate constant of forward reaction in aqueous phase (cm ³ /(mol s))
k_{aq-2}	second order rate constant of backward reaction in aqueous phase (cm ³ /(mol s))
k_{org-1}	second order rate constant of forward reaction in organic phase (cm ³ /(mol s))
k_{org-2}	second order rate constant of backward reaction in organic phase (cm ³ /(mol s))
K_{QCN}	distribution coefficient of QCN between the aqueous and organic phase (dimensionless)
K_{QI}	distribution coefficient of QI between the aqueous and organic phase (dimensionless)
K_{QX}	distribution coefficient of QX between the aqueous and organic phase (dimensionless)
$N_{CN^-}^{total}$	total moles of NaCN added (mol)
$N_{I^-}^{total}$	total moles of I ⁻ added (mol)
N_{Qaq}	moles of catalyst in the aqueous phase (mol)
N_{Qorg}	moles of catalyst in the organic phase (mol)
N_{Qtotal}	total moles of catalyst added (mol)
$[QCN]_{aq}$	concentration of tetrabutylammonium cyanide in the aqueous phase (mol/cm ³)
$[QCN]_{org}$	concentration of tetrabutylammonium cyanide in the organic phase (mol/cm ³)
$[QI]_{aq}$	concentration of TBAI in the aqueous phase (mol/cm ³)
$[QI]_{org}$	concentration of TBAI in the organic phase (mol/cm ³)
$[QX]_{aq}$	concentration of TBAB in the aqueous phase (mol/cm ³)
$[QX]_{org}$	concentration of TBAB in the organic phase (mol/cm ³)

$[RCN]_{org}$	concentration of <i>p</i> -CBCN in the organic phase (mol/cm ³)
$[RI]_{org}$	concentration of <i>p</i> -CBI in the organic phase (mol/cm ³)
$[RX]_{org}$	concentration of <i>p</i> -CBC in the organic phase (mol/cm ³)
V_{aq}	volume of aqueous phase (cm ³)
V_{org}	volume of organic phase (cm ³)
X_A	fractional conversion of reactant A

significantly increase reaction rates, alter product distributions or increase catalyst stability [6].

The current study endeavours to explore the role of potassium iodide (KI) as a co-catalyst to enhance the rate of cyanide displacement reaction on *p*-chlorobenzyl chloride, to investigate the several empirical factors that influence the catalytic activity under L–L PTC conditions and to examine the kinetic and modelling aspects of the process based on reaction mechanism.

2. Experimental methods

2.1. Procedure

The reactions were studied in a 5 cm i.d. fully-baffled mechanically agitated contactor of 100 cm³ total capacity, which was equipped with a six-blade pitched turbine impeller and a reflux condenser. The reactor was kept in an isothermal oil bath whose temperature was maintained at a desired value and the reaction mixture was agitated mechanically with the help of an electric motor.

Typical runs were conducted with 0.025 mol of *p*-chlorobenzyl chloride dissolved in toluene to make up volume of organic phase to 25 cm³. Since, the objective was to have all sodium cyanide consumed, to circumvent its disposal problems, it was used in a stoichiometrically deficient quantity. Therefore, 0.02 mol of sodium cyanide (25 cm³ aqueous solution corresponding to a concentration of 0.8×10^{-3} mol/cm³(aq)) was used. Thus, the maximum conversion of *p*-chlorobenzyl chloride was limited to 80%. A total amount of 0.002 mol each of the catalyst tetrabutylammonium bromide (TBAB)

and co-catalyst KI were used. All standard reactions were conducted at 90 °C.

2.2. Analysis

Samples of the organic phase were withdrawn periodically and analysed by gas chromatography [Chemito Model 8510]. A 2.0 m × 3.2 mm i.d. stainless steel column packed with 10% OV-17 on Chromosorb WHP was used for analysis in conjunction with a flame ionisation detector. Synthetic mixtures were prepared for calibration and used to calculate the concentrations of *p*-chlorobenzyl chloride and *p*-chlorophenyl acetonitrile quantitatively. The rates of reaction were based on the disappearance of *p*-chlorobenzyl chloride. The sole product, *p*-chlorophenyl acetonitrile was confirmed by GC–MS analysis.

3. Results and discussion

3.1. Proposed mechanism

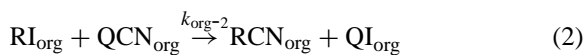
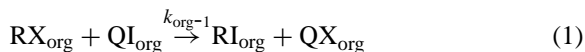
The various steps envisaged in the reaction mechanism for L–L PTC reaction are as shown in Scheme 1. In the aqueous phase, the quaternary cation Q^+ ex-

ists as two ion-pairs, viz. Q^+I^- and a finite quantity of Q^+CN^- , which are instantaneously extracted into the organic phase due to the high organophilicity of the catalyst cation. In the organic phase, the reactant *p*-chlorobenzyl chloride is converted to the more reactive iodide form, regenerating the catalyst (Q^+X^-) in the process. *p*-Chlorobenzyl iodide, thus formed reacts with the active species Q^+CN^- to give the product *p*-chlorophenyl acetonitrile. Thus, enhanced reaction rates are observed due to the in situ formation of the more reactive *p*-chlorobenzyl iodide owing to the co-catalytic action of KI.

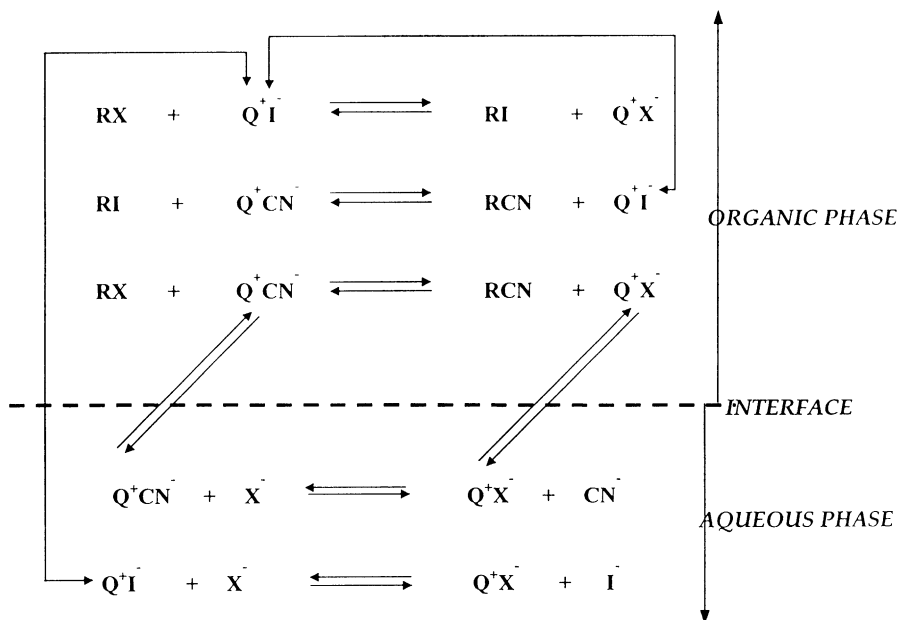
3.2. Derivation of the rate equation

Based on Scheme 1, the following equations are envisaged:

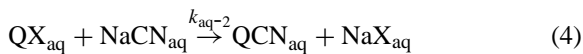
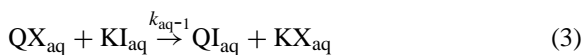
Organic phase reactions:



Aqueous phase reactions:



Scheme 1. Mechanism of liquid–liquid phase transfer catalysed synthesis of *p*-chlorophenyl acetonitrile co-catalysed by potassium iodide.



Mass transfer across the interface:



Equilibrium constants:

$$K_{\text{QI}} = \frac{[\text{QI}]_{\text{org}}}{[\text{QI}]_{\text{aq}}}, \quad K_{\text{QX}} = \frac{[\text{QX}]_{\text{org}}}{[\text{QX}]_{\text{aq}}},$$

$$K_{\text{QCN}} = \frac{[\text{QCN}]_{\text{org}}}{[\text{QCN}]_{\text{aq}}} \quad (8)$$

Catalyst distribution: The total quantity of catalyst added $N_{\text{Q}_{\text{total}}}$ is distributed in both the phases in six different ion-pairs namely, $[\text{QCN}]_{\text{org}}$, $[\text{QX}]_{\text{org}}$, $[\text{QI}]_{\text{org}}$, $[\text{QCN}]_{\text{aq}}$, $[\text{QX}]_{\text{aq}}$ and $[\text{QI}]_{\text{aq}}$. If it is assumed that the distribution of the cation Q^+ in the organic and aqueous phase is constant then the various exchanges which take place in the respective phases need to be considered.

Thus,

$$N_{\text{Q}_{\text{total}}} = \text{total moles of catalyst added} = N_{\text{Q}_{\text{org}}} + N_{\text{Q}_{\text{aq}}}$$

$$N_{\text{Q}_{\text{total}}} = \{[\text{QI}]_{\text{org}} + [\text{QCN}]_{\text{org}} + [\text{QX}]_{\text{org}}\} V_{\text{org}} + \{[\text{QI}]_{\text{aq}} + [\text{QCN}]_{\text{aq}} + [\text{QX}]_{\text{aq}}\} V_{\text{aq}} \quad (9)$$

$$N_{\text{Q}_{\text{total}}} = [\text{QI}]_{\text{org}} \left\{ V_{\text{org}} + \frac{[\text{QI}]_{\text{aq}} V_{\text{aq}}}{[\text{QI}]_{\text{org}}} \right\} + [\text{QCN}]_{\text{org}} \left\{ V_{\text{org}} + \frac{[\text{QCN}]_{\text{aq}} V_{\text{aq}}}{[\text{QCN}]_{\text{org}}} \right\} + [\text{QX}]_{\text{org}} \left\{ V_{\text{org}} + \frac{[\text{QX}]_{\text{aq}} V_{\text{aq}}}{[\text{QX}]_{\text{org}}} \right\} \quad (10)$$

Substituting for $[\text{QI}]_{\text{org}}$, $[\text{QCN}]_{\text{org}}$ and $[\text{QX}]_{\text{org}}$ in terms of equilibrium constants from Eq. (8):

$$N_{\text{Q}_{\text{total}}} = [\text{QI}]_{\text{org}} \left\{ V_{\text{org}} + \frac{V_{\text{aq}}}{K_{\text{QI}}} \right\} + [\text{QCN}]_{\text{org}} \left\{ V_{\text{org}} + \frac{V_{\text{aq}}}{K_{\text{QCN}}} \right\} + [\text{QX}]_{\text{org}} \left\{ V_{\text{org}} + \frac{V_{\text{aq}}}{K_{\text{QX}}} \right\} \quad (11)$$

$$[\text{QI}]_{\text{org}} = \alpha N_{\text{Q}_{\text{total}}} - \beta [\text{QCN}]_{\text{org}} - \gamma [\text{QX}]_{\text{org}} \quad (12)$$

Where

$$\alpha = \frac{1}{\{V_{\text{org}} + V_{\text{aq}}/K_{\text{QI}}\}} \quad (13)$$

$$\beta = \frac{\{V_{\text{org}} + V_{\text{aq}}/K_{\text{QCN}}\}}{\{V_{\text{org}} + V_{\text{aq}}/K_{\text{QI}}\}} = \alpha \left\{ V_{\text{org}} + \frac{V_{\text{aq}}}{K_{\text{QCN}}} \right\} \quad (14)$$

$$\gamma = \frac{\{V_{\text{org}} + V_{\text{aq}}/K_{\text{QX}}\}}{\{V_{\text{org}} + V_{\text{aq}}/K_{\text{QI}}\}} = \alpha \left\{ V_{\text{org}} + \frac{V_{\text{aq}}}{K_{\text{QX}}} \right\} \quad (15)$$

From Eq. (1), the rate of reaction within the organic phase,

$$-\frac{d[\text{RX}]_{\text{org}}}{dt} = k_{\text{org-1}} [\text{RX}]_{\text{org}} [\text{QI}]$$

Substituting for $[\text{QI}]_{\text{org}}$ from Eq. (12),

$$-\frac{d[\text{RX}]_{\text{org}}}{dt} = k_{\text{org-1}} [\text{RX}]_{\text{org}} \{ \alpha N_{\text{Q}_{\text{total}}} - \beta [\text{QCN}]_{\text{org}} - \gamma [\text{QX}]_{\text{org}} \} \quad (16)$$

Let $[\text{RX}]_{\text{org}} = [\text{A}]$

Since,

$$[\text{A}] = [\text{A}]_0 (1 - X_A) \quad (17)$$

$$-\frac{d[\text{A}]}{dt} = [\text{A}]_0 \frac{dX_A}{dt} \quad (18)$$

Therefore Eq. (16) becomes

$$[\text{A}]_0 \frac{dX_A}{dt} = k_{\text{org-1}} [\text{A}]_0 (1 - X_A) \times \{ \alpha N_{\text{Q}_{\text{total}}} - \beta [\text{QCN}]_{\text{org}} - \gamma [\text{QX}]_{\text{org}} \} \quad (19)$$

Upon separation of variables, we get

$$\frac{dX_A}{(1 - X_A)} = k_{\text{org-1}} \{ \alpha N_{\text{Q}_{\text{total}}} - \beta [\text{QCN}]_{\text{org}} - \gamma [\text{QX}]_{\text{org}} \} dt \quad (20)$$

An order of magnitude analysis can now be performed:

The total moles of catalyst added to the reaction mixture ($N_{Q_{total}}$) are only 10% of the limiting reactant (NaCN) taken in the aqueous phase. This catalyst is distributed among six ion-pairs and depending on the distribution of these ion-pairs between the organic and aqueous phase, the catalyst cation (Q^+) can combine in appropriate proportions with different anions. Considering the preferential distribution of tetrabutylammonium cation in the organic phase, 90% of the total catalyst added can be assumed to be in the organic phase and remaining 10% in the aqueous phase. Of the 90% catalyst in the organic phase, about 90% will be taken up by Q^+I^- because of the tendency of iodide anion to associate strongly with the quaternary cation in the organic phase and the remaining 10% will be distributed between Q^+CN^- and Q^+X^- . So, effectively only 11% of the total catalyst added or only 1% catalyst with respect to the reactant RX (A) is in the Q^+CN^- and Q^+X^- form. Hence, any variation in Q^+CN^- and Q^+X^- concentration with respect to the reactant will be negligible and can be assumed to be constant.

So, if $[QCN]_{org}$ and $[QX]_{org}$ are not functions of time, then integrating Eq. (20), we get

$$-\ln(1 - X_A) = k_{org-1}t\{\alpha N_{Q_{total}} - \beta[QCN]_{org} - \gamma[QX]_{org}\} \quad (21)$$

Substituting from Eq. (12):

$$-\ln(1 - X_A) = k_{org-1}[QI]_{org}t \quad (22)$$

4. Validation of the model

In order to verify the proposed mechanism of the reaction and validate the model, the effects of various parameters on the rates of reaction were studied.

4.1. Effect of different catalysts

There was no reaction in the absence of any catalyst. Various catalysts such as TBAB, tetrabutylammonium hydrogen sulphate (TBAHS) and ethyltriphenylphosphonium bromide (ETPPB) were employed under otherwise similar experimental conditions. TBAB was also employed with a co-catalyst KI (Fig. 1).

Of all the catalysts tested, TBAB–KI combination was observed to have substantially greater catalytic

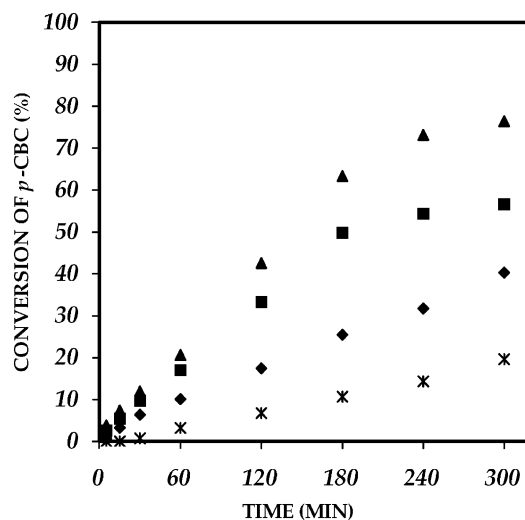


Fig. 1. Effect of different catalysts: *p*-CBC, 0.025 mol; NaCN, 0.02 mol. Toluene, 25 cm³; H₂O, 25 cm³. Catalyst, 0.002 mol. Temperature, 90 °C; speed of agitation, 1500 rpm. (▲) TBAB–KI, (■) TBAHS, (×) TBAB, (◆) ETPPB.

activity than TBAB, ETPPB and TBAHS. This can be explained by the in situ generation of TBAI by the anion exchange between TBAB and co-catalyst KI. So, the actual catalytic species is TBAI. ETPPB displays moderate activity in this reaction. As for the other catalysts, the cation TBA^+ of the quaternary ammonium salts is a soft acid and the reactivity of the catalysts is determined by the anions. In the two-phase system of water and toluene, the order of the bonding force of the anions formed with TBA^+ in the aqueous phase is $I^- > Br^- > HSO_4^-$. A catalyst of soft acid–hard base being of high energy level, TBA^+ easily reacts with the nucleophilic anion to form an ion pair in the aqueous phase. The ion pair then transfers to the organic phase to facilitate the displacement reaction. Between Br^- and HSO_4^- the bonding of the latter being weak, it facilitates the formation of a reactive ion-pair with the nucleophilic anion in the aqueous phase and, hence the conversion is better with TBAHS than with TBAB. The case is, however, different with TBAI. Even though I^- is a soft base and has a strong bonding force with TBA^+ , TBAI is a compound of low energy level and it restricts the transfer of TBA^+ with nucleophilic anion to the organic phase. However, TBAI is strongly nucleophilic and reacts with benzyl chloride to form active benzyl iodide and nucleophilic TBACl, which is easily trans-

ferred to the aqueous phase. Thus, the enhanced reactivity of TBAB–KI could be attributed to the exchange of anions to generate TBAI in situ, since the quaternary ammonium cation prefers to be associated with the iodide relative to the chloride. Therefore, TBAB along with co-catalyst KI was used in subsequent part of this study for reactions under L–L conditions.

4.2. Effect of phase:volume ratio

The effect of phase:volume ratio was studied for 1.5:1, 1:1 and 1:1.5 ratios of organic phase to aqueous phase volumes under otherwise similar experimental conditions. The moles of all reactants and catalyst added were also kept constant. It is seen from Fig. 2, that when the volume ratio of organic to aqueous phase was 1:1.5, the partitioning of Q^+CN^- in the organic phase was the least and, hence, conversions were the lowest. When the phase ratio of the organic to aqueous phase was fixed at 1:1, the best conversion values were obtained. Under these conditions, it was observed that organic phase was the dispersed phase and the aqueous phase was the continuous phase. The lower conversions for 1.5:1 and 1:1.5 volume ratios could be due to increase in dilution of the reactants and

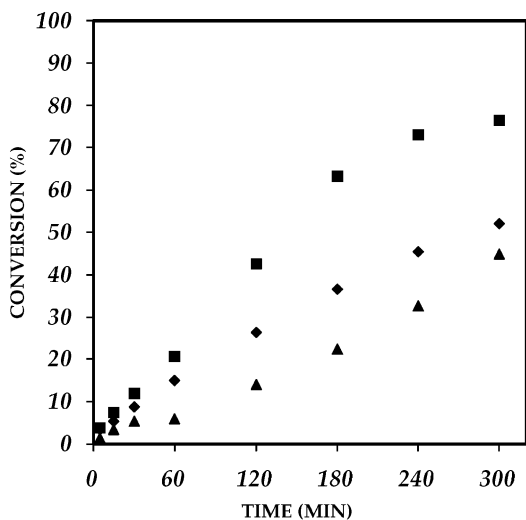


Fig. 2. Effect of phase volume ratio (org:aq): TBAB, 0.002 mol; KI, 0.002 mol. *p*-CBC, 0.025 mol; NaCN, 0.02 mol. Temperature, 90 °C; speed of agitation, 1500 rpm. Organic to aqueous phase volume ratio (■) 1:1, (◆) 1.5:1, (▲) 1:1.5.

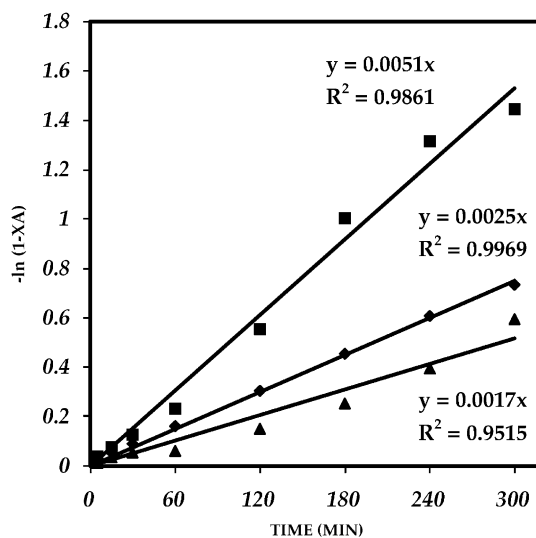


Fig. 3. Kinetic plot for the effect of phase volume ratio: *p*-CBC, 0.025 mol; NaCN, 0.02 mol. TBAB, 0.002 mol; KI, 0.002 mol. Temperature, 90 °C; speed of agitation: 1500 rpm. Organic to aqueous phase volume ratio (■) 1:1, (◆) 1.5:1, (▲) 1:1.5.

also due to the unfavourable distribution of the catalyst. So, further experiments were conducted by using equal volumes of the phases. The proposed model is valid for various ratios of phase:volume as is seen from a plot of $-\ln(1 - X_A)$ versus time as shown in Fig. 3.

4.3. Effect of speed of agitation

The effect of speed of agitation on the conversion of *p*-chlorobenzyl chloride was studied at 700, 1000 and 1500 rpm (Fig. 4). The conversion was found to increase with an increase in the speed of agitation from 700 to 1000 rpm due to the formation of small droplets leading to more surface area for mass transfer. However, at 1000 and 1500 rpm the conversion was found to be practically the same because no further change in droplet size was possible. In the case of L–L PTC, the droplets of the dispersed phase will have a limited size at higher speeds, which remains constant and, hence the mass transfer area becomes steady beyond 1500 rpm. Thus, a speed of agitation of 1500 rpm was employed to eliminate the external mass transfer resistance and for assessing the effect of other variables on the rate of reaction.

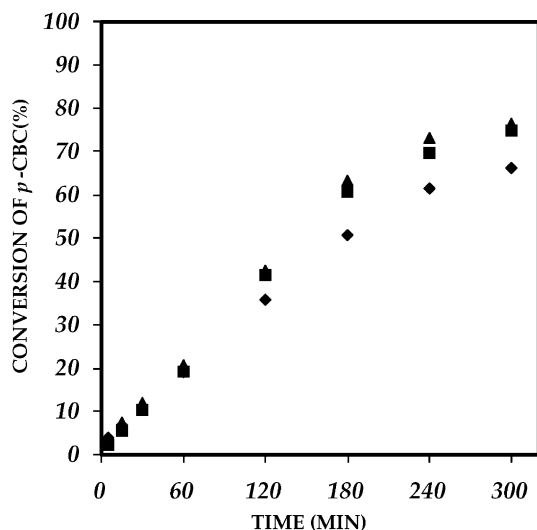


Fig. 4. Effect of speed of agitation (rpm): (◆) 700, (■) 1000, (▲) 1500. *p*-CBC, 0.025 mol; NaCN, 0.02 mol. TBAB, 0.002 mol; KI, 0.002 mol. Toluene, 25 cm³; H₂O, 25 cm³. Temperature, 90 °C.

4.4. Effect of catalyst concentration

The amount of catalyst (TBAB) was varied from 0.001 to 0.004 mol with an equimolar quantity of KI under otherwise similar experimental conditions. The conversion of *p*-chlorobenzyl chloride is plotted against time for different catalyst concentrations (Fig. 5). It is observed that as the catalyst loading is increased there is an increase in conversion, due to the fact that concentration of Q⁺CN⁻ extracted into the organic phase increases with increasing catalyst concentration. Fig. 6 shows that a plot of $-\ln(1 - X_A)$ versus time is a straight line passing through origin from which we get the slope

$$k_{p1} = k_{org-1} \{ \alpha N_{Q_{total}} - \beta [QCN]_{org} - \gamma [QX]_{org} \} \quad (23)$$

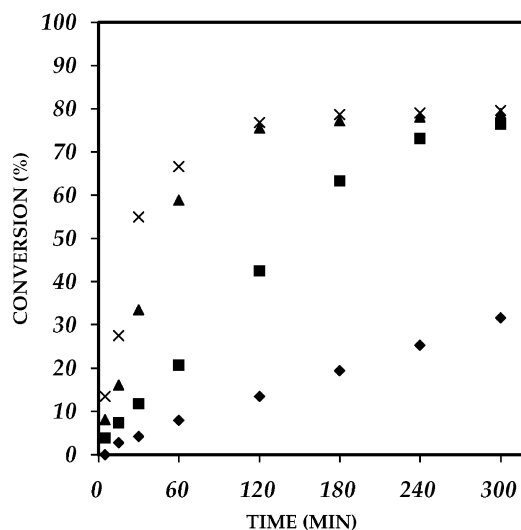
In reference to Eq. (23) for different moles of the catalyst $N_{Q_{total}}$, a plot of k_{p1} versus $N_{Q_{total}}$ will give a straight line with

$$\text{slope} = k_{org-1} \alpha \quad (24)$$

and *Y*-intercept

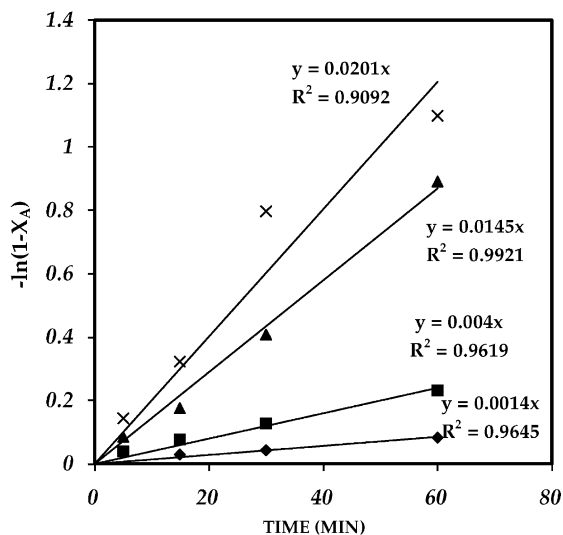
$$= -k_{org-1} \{ \beta [QCN]_{org} + \gamma [QX]_{org} \} \quad (25)$$

Here, the *X*-intercept, when $k_{p1} = 0$, give us



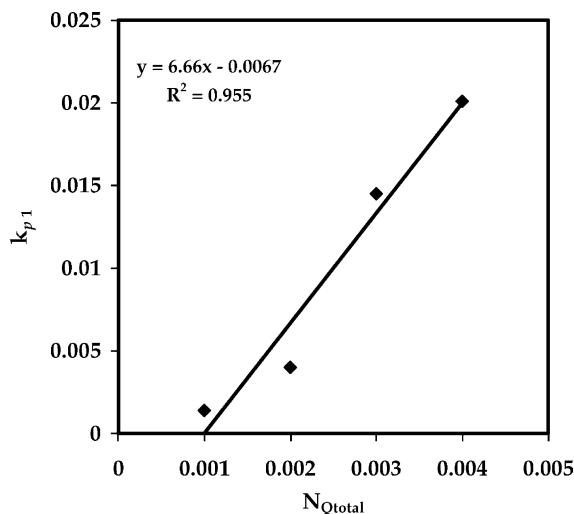
(With equimolar quantity of KI in each case)

Fig. 5. Effect of catalyst (TBAB) concentration: (×) 0.004 mol, (▲) 0.003 mol, (■) 0.002 mol, (◆) 0.001 mol (with equimolar quantity of KI in each case). *p*-CBC, 0.025 mol; NaCN, 0.02 mol. Toluene, 25 cm³; H₂O, 25 cm³. Temperature, 90 °C; speed of agitation, 1500 rpm.



(With equimolar quantity of KI in each case)

Fig. 6. Kinetic plot for the effect of catalyst (TBAB) concentration: (×) 0.004 mol, (▲) 0.003 mol, (■) 0.002 mol, (◆) 0.001 mol (with equimolar quantity of KI in each case).

Fig. 7. Plot of k_{p1} vs. $N_{Q_{total}}$.

$$k_{org-1} \{ \alpha N_{Q_{total}} - \beta [QCN]_{org} - \gamma [QX]_{org} \} = 0 \quad \text{at} \\ N_{Q_{total}} = 0.001 \quad (26)$$

as is observed in Fig. 7.

So, from the above Eqs. (24)–(26), $[QCN]_{org}$ and $[QX]_{org}$ can be evaluated if α , β and γ are known. In other words, K_{QX} , K_{QCN} and K_{QI} should be independently known.

4.5. Effect of co-catalyst concentration

Experiments were conducted by varying the co-catalyst (KI) quantity from 0.001 to 0.003 mol but keeping amount of catalyst TBAB constant at 0.002 mol. In the absence of co-catalyst the conversions were found to be very low (Fig. 1). The conversion was found to increase with an increase in co-catalyst concentration (Fig. 8). The co-catalyst, which is added in stoichiometric quantities to that of the catalyst, exchanges its iodide anion with the bromide ion of TBAB to form TBAI in situ. The quaternary ammonium iodide, located in organic phase, reacts with *p*-chlorobenzyl chloride to form the more reactive *p*-chlorobenzyl iodide. The quaternary ammonium chloride formed during this reaction is partitioned into the aqueous phase, where an exchange reaction ensues in which the quaternary cation Q^+ pairs with the organic anion CN^- . This is followed

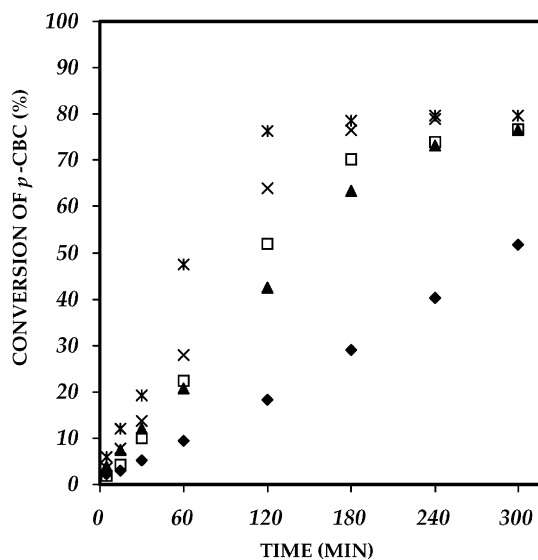


Fig. 8. Effect of co-catalyst (KI) concentration: (X) 0.003 mol, (x) 0.0025 mol, (▲) 0.002 mol, (◆) 0.001 mol, (□) 0.002 mol of TBAI. *p*-CBC, 0.025 mol; NaCN, 0.02 mol. TBAB, 0.002 mol. Toluene, 25 cm³; H₂O, 25 cm³. Temperature, 90 °C; speed of agitation, 1500 rpm.

by the partitioning of the ion pair Q^+CN^- into the organic phase, where it reacts with *p*-chlorobenzyl iodide to form the product and quaternary ammonium iodide and, thus the catalytic cycle continues. Due to this salting out effect as well as the formation of benzyl iodide, the overall reaction rate increased as expected. This mechanism is further confirmed by the observation that when TBAI is employed as the catalyst, the conversion is practically the same as that for TBAB–KI combination.

Again, the variation in the concentration of KI will affect $[QI]_{org}$, $[QI]_{aq}$ and $[RI]_{org}$, since I^- is distributed as QI and RI in the organic phase. It can, therefore, be shown that: if $N_{I_{total}}^-$ are the total moles added,

$$N_{I_{total}}^- = [QI]_{aq} V_{aq} + [QI]_{org} V_{org} + [RI]_{org} V_{org} \quad (27)$$

$$N_{I_{total}}^- = [QI]_{org} V_{org} \left[1 + \frac{V_{aq}}{K_{QI} V_{org}} \right] + [RI]_{org} V_{org} \quad (28)$$

$$[QI]_{org} = \frac{N_{I_{total}}^- / V_{org} - [RI]_{org}}{\left[1 + V_{aq} / K_{QI} V_{org} \right]} \quad (29)$$

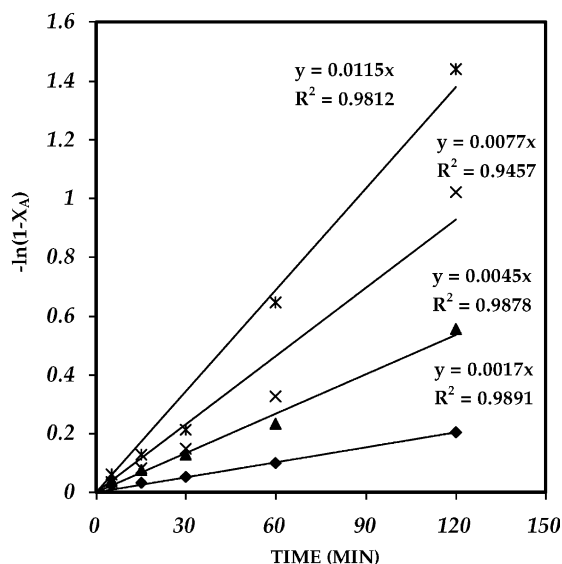


Fig. 9. Kinetic plot for the effect of co-catalyst (KI) concentration: (x) 0.003 mol, (x) 0.0025 mol, (▲) 0.002 mol, (◆) 0.001 mol. *p*-CBC, 0.025 mol; NaCN, 0.02 mol. TBAB, 0.002 mol. Toluene, 25 cm³; H₂O, 25 cm³. Temperature, 90 °C.

Substituting for in $[QI]_{org}$ in Eq. (22), we get:

$$-\ln(1 - X_A) = k_{org-1} \left\{ \frac{N_{I_{total}^-} / V_{org}}{[1 + V_{aq} / K_{QI} V_{org}]} - \frac{[RI]_{org}}{[1 + V_{aq} / K_{QI} V_{org}]} \right\} t \quad (30)$$

$$-\ln(1 - X_A) = k_{org-1} \{ aN_{I_{total}^-} - b[RI]_{org} \} t \quad (31)$$

Again any variation in $[RI]_{org}$ concentration with respect to the reactant $[RX]_{org}$, will be negligible and can be assumed to be constant.

Therefore, a plot of $-\ln(1 - X_A)$ versus t for the varying co-catalyst concentration will be a straight line (Fig. 9) from which we get the slope:

$$k_{p2} = k_{org-1} \{ aN_{I_{total}^-} - b[RI]_{org} \} \quad (32)$$

A plot of k_{p2} versus $N_{I_{total}^-}$ will give a profile similar to that obtained for catalyst concentration (Fig. 10).

4.6. Effect of *p*-chlorobenzyl chloride concentration

The concentration of *p*-chlorobenzyl chloride was varied from 4×10^{-4} to 1.2×10^{-3} mol/cm³ under

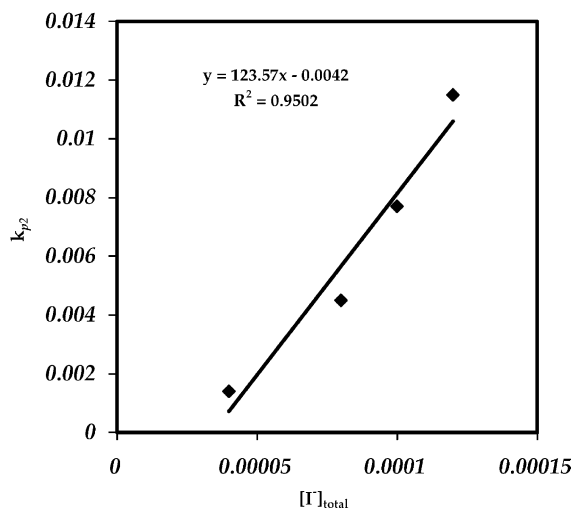


Fig. 10. Plot of K_{p2} vs. $[I^-]_{total}$.

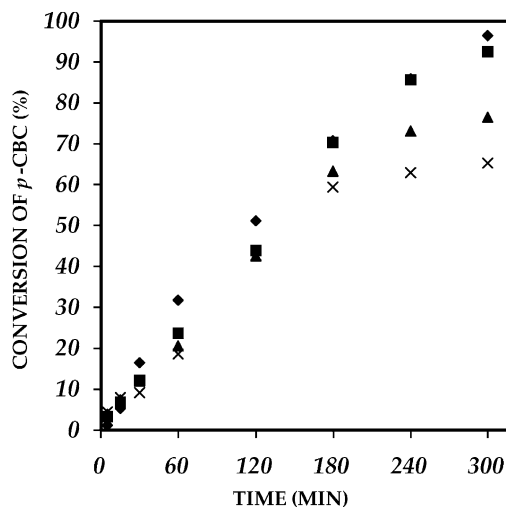
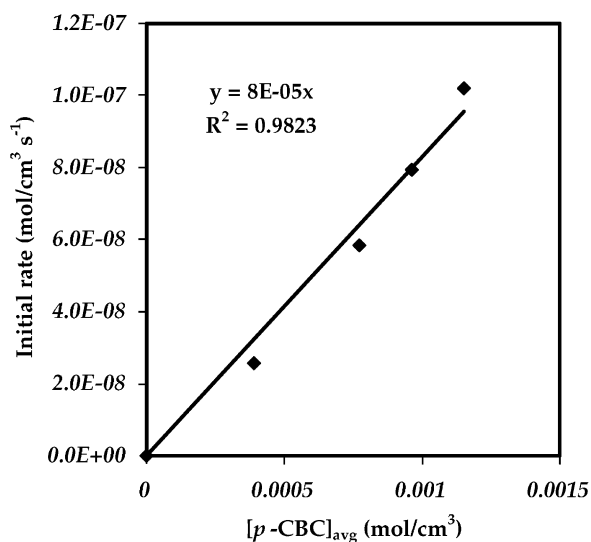
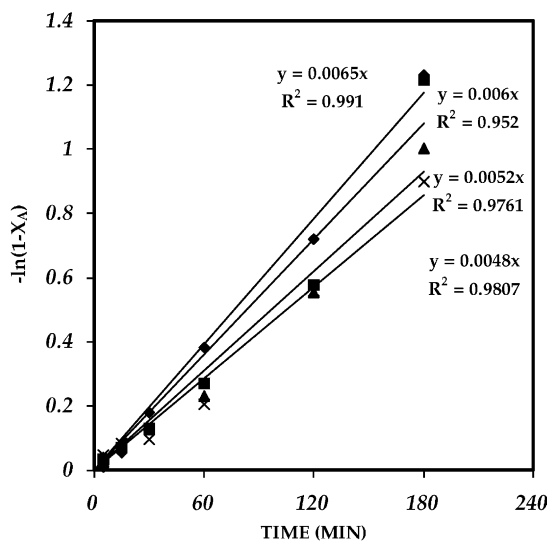


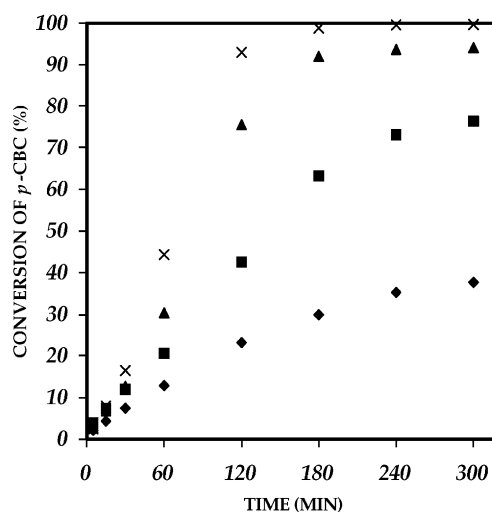
Fig. 11. Effect of *p*-CBC concentration: (◆) 0.01 mol, (■) 0.02 mol, (▲) 0.025 mol, (x) 0.03 mol. NaCN, 0.02 mol; TBAB, 0.002 mol; KI, 0.002 mol. Toluene, 25 cm³; H₂O, 25 cm³. Temperature, 90 °C; speed of agitation, 1500 rpm.

otherwise similar experimental conditions. Fig. 11 shows that the conversion of *p*-CBC decreases with an increase in concentration of *p*-CBC. However, the initial rates of reaction increase with an increase in average initial concentration of *p*-CBC as is seen from Fig. 12. Again the validity of the model was tested for various values of *p*-CBC by plotting $-\ln(1 - X_A)$ versus t (Fig. 13).

Fig. 12. Plot of initial rate vs. $[p\text{-CBC}]_{\text{avg}}$.Fig. 13. Kinetic plot for the effect of $p\text{-CBC}$ concentration: (◆) 0.01 mol, (■) 0.02 mol, (▲) 0.025 mol, (×) 0.03 mol. NaCN, 0.02 mol; TBAB, 0.002 mol; KI, 0.002 mol. Toluene, 25 cm³; H₂O, 25 cm³. Temperature, 90 °C; speed of agitation, 1500 rpm.

4.7. Effect of nucleophile concentration

The effect was studied by varying sodium cyanide concentration from 4×10^{-4} to 1.2×10^{-3} mol/cm³. As seen from Fig. 14, as the concentration of the

Fig. 14. Effect of NaCN concentration: (×) 0.03 mol, (▲) 0.025 mol, (■) 0.02 mol, (◆) 0.01 mol. $p\text{-CBC}$, 0.025 mol; TBAB, 0.002 mol; KI, 0.002 mol. Toluene, 25 cm³; H₂O, 25 cm³. Temperature, 90 °C; speed of agitation, 1500 rpm.

nucleophile increases the conversion increases, since more and more nucleophile in the Q^+CN^- form is available for the reaction. Although quantitative conversion could be obtained by using higher concentration of NaCN, stoichiometrically deficient quantity of 0.02 mol was used for all the reactions to avoid disposal problems.

NaCN material balance is taken:

there are free CN^- ions in the aqueous phase and the rest as QCN_{aq} and QCN_{org} .

$$N_{\text{CN}^-}_{\text{total}} = [CN]_{\text{aq}} V_{\text{aq}} + [QCN]_{\text{aq}} V_{\text{aq}} + [QCN]_{\text{org}} V_{\text{org}} \quad (33)$$

$$N_{\text{CN}^-}_{\text{total}} = [CN]_{\text{aq}} V_{\text{aq}} + [QCN]_{\text{org}} \frac{V_{\text{aq}}}{K_{\text{QCN}}} + [QCN]_{\text{org}} V_{\text{org}} \quad (34)$$

$$[QCN]_{\text{org}} = \frac{(N_{\text{CN}^-}_{\text{total}} - [CN]_{\text{aq}} V_{\text{aq}})}{V_{\text{org}} (1 + V_{\text{aq}}/K_{\text{QCN}})} \quad (35)$$

Thus, it is obvious that when the cyanide concentration is increased, the rate of reaction will increase.

For a given quantity of catalyst added, N_{Qtotal} , the variation in the concentration of NaCN added to the aqueous phase should affect only $[QCN]_{\text{org}}$ in the

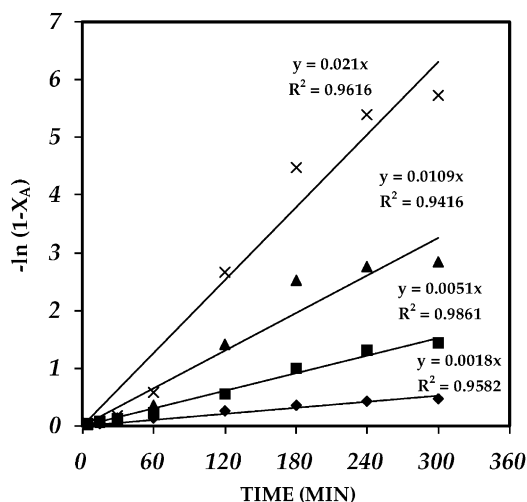


Fig. 15. Kinetic plot for the effect of NaCN concentration: (x) 0.03 mol, (▲) 0.025 mol, (■) 0.02 mol, (◆) 0.01 mol. *p*-CBC, 0.025 mol; TBAB, 0.002 mol; KI, 0.002 mol. Toluene, 25 cm³; H₂O, 25 cm³. Temperature, 90 °C; speed of agitation, 1500 rpm.

Eq. (21) as $[QCN]_{org}$ will be directly proportional to $[NaCN]_{aq}$. Therefore, a plot of $-\ln(1 - X_A)$ versus t will give a straight line as shown in Fig. 15 with a slope of

$$k_{p3} = k_{org-1} \{ \alpha N_{Q_{total}} - \beta [QCN]_{org} - \gamma [QX]_{org} \} \quad (36)$$

A plot of k_{p3} versus $[NaCN]_{aq}$ will give a profile similar to that obtained for catalyst concentration. This is seen from Fig. 16.

The similar trend, which is obtained for Figs. 7, 10 and 16, demonstrate that there is internal consistency in the data and that the assumptions considered for derivation of the equation are correct. Thus, the above theory is validated against experimental data. Further knowing the actual values of distribution coefficients of various catalytic species K_{QI} , K_{QX} and K_{QCN} under the present experimental conditions, the exact values for k_{org-1} , $[QCN]_{org}$ and $[QX]_{org}$ can be calculated.

4.8. Effect of temperature

The effect of temperature on the rate of the reaction of *p*-chlorobenzyl chloride was studied in the range of 70–100 °C. The conversion of *p*-chlorobenzyl chloride was observed to increase with an increase in the reac-

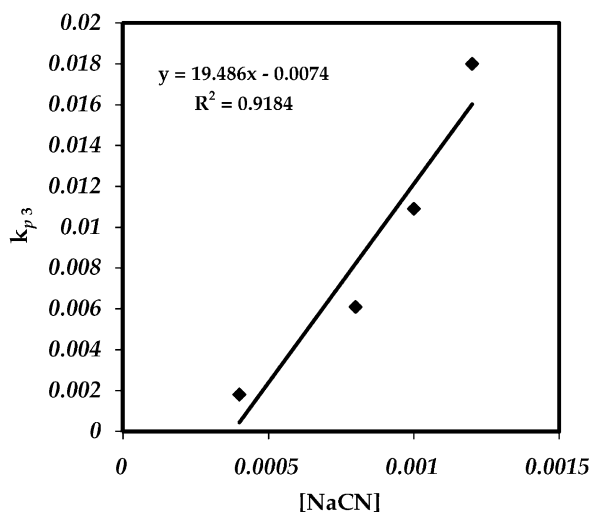


Fig. 16. Plot of k_{p3} vs. $[NaCN]$.

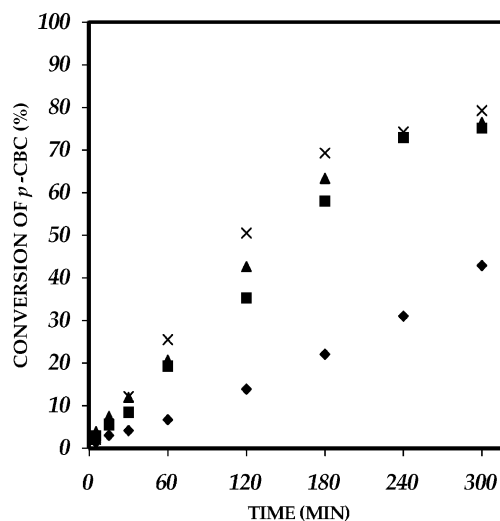


Fig. 17. Effect of temperature: (x) 100 °C, (▲) 90 °C, (■) 80 °C, (◆) 70 °C. *p*-CBC, 0.025 mol; NaCN, 0.02 mol. TBAB, 0.002 mol; KI, 0.002 mol. Toluene, 25 cm³; H₂O, 25 cm³. Speed of agitation: 1500 rpm.

tion temperature. The increase is substantial when the temperature is increased from 70 to 80 °C. For reactions beyond 80 °C, there was a marginal difference in the final conversions (Fig. 17). A plot of $-\ln(1 - X_A)$ versus t gives a straight line as shown in Fig. 18. The apparent activation energy from the Arrhenius plot was found to be 9.87 kcal/mol (Fig. 19).

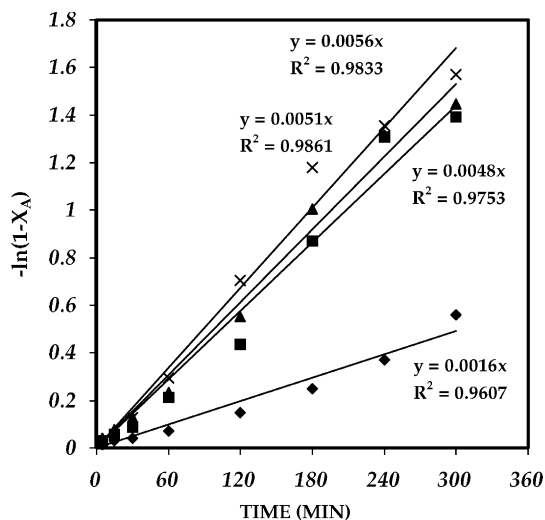


Fig. 18. Kinetic plot for the effect of temperature: (x) 100 °C, (▲) 90 °C, (■) 80 °C, (◆) 70 °C. *p*-CBC, 0.025 mol; NaCN, 0.02 mol. TBAB, 0.002 mol; KI, 0.002 mol. Toluene, 25 cm³; H₂O, 25 cm³. Speed of agitation, 1500 rpm.

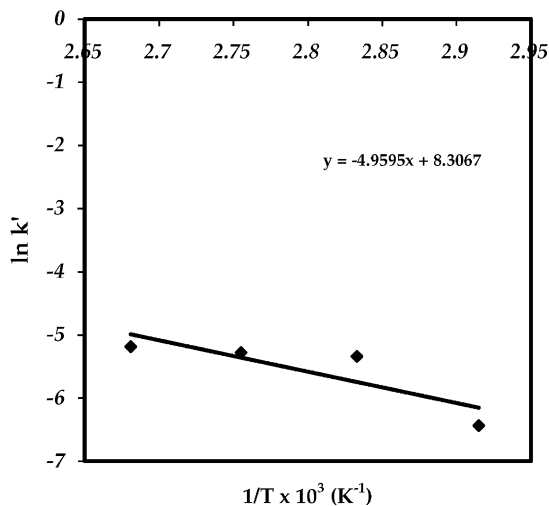


Fig. 19. Arrhenius plot.

5. Conclusions

The L–L PTC cyanide displacement reaction on *p*-chlorobenzyl chloride to synthesise *p*-chlorophenyl acetonitrile was studied by using TBAB as the catalyst along with potassium iodide as the co-catalyst at 90 °C. The selectivity of the process is 100%. The mechanism of the reaction involves in situ formation of *p*-chlorobenzyl iodide in the presence of KI as co-catalyst, which leads to enhanced reaction rates. The catalyst is predominantly distributed in two forms Q⁺I⁻ and Q⁺CN⁻. A kinetic model is developed to account for the experimental observations. The product is industrially valuable.

Acknowledgements

G.D. Yadav acknowledges CSIR and AICTE, New Delhi and the Darbari Seth Professorship Endowment for the research support. Y.B. Jadhav acknowledges AICTE and Ambuja Cements for the award of a JRF and SRF, respectively. G.D. Yadav is grateful to the Michigan State University for providing excellent facilities as the Johansen Crosby Visiting Chair Professor of Chemical Engineering during 2001–2002.

References

- [1] F. Masuko, S. Hasegawa, S. Nakai, Jpn. Kokai 78 31 642 (1978); Chem. Abstr. 89 (1978) 108744.
- [2] B.V. Maatschappi, Jpn. Kokai Tokkyo Koho 81 20 561 (1981); Chem. Abstr. 95 (1981) 6869.
- [3] P.A. Verbrugge, E.W. Uurbanus, P.A. Kramer, W. Terlouw, British Patent 1 528 043; Chem. Abstr. 91 (1979) 123576
- [4] S.S. Shavanov, G.A. Tolstikov, G.A. Viktorov, Zh. Obshch. Khim. 59 (1989) 1615; S.S. Shavanov, G.A. Tolstikov, G.A. Viktorov, Chem. Abstr. 112 (1990) 76064.
- [5] S.L. Regen, J. Org. Chem. 42 (1977) 875.
- [6] C.M. Starks, C.L. Liotta, M. Halpern, Phase-Transfer Catalysis: Fundamentals, Applications and Industrial Perspectives, Chapman & Hall, New York, 1994.